HHS Public Access

Author manuscript

FEBS J. Author manuscript; available in PMC 2021 February 01.

Published in final edited form as:

FEBS J. 2020 February ; 287(3): 452–464. doi:10.1111/febs.15040.

Proteolytic and Nonproteolytic Activation Mechanisms Result in Conformationally and Functionally Different Forms of Coagulation Factor XIII A

Boris A. Anokhin[1], **William L. Dean**[2,3,4], **Kerrie A. Smith**[5], **Matthew J. Flick**[6], **Robert A.S. Ariëns**[5], **Helen Philippou**[5], **Muriel C. Maurer**[1]

[1]Department of Chemistry, University of Louisville, Louisville, KY, USA

[2]Brown Cancer Center, University of Louisville School of Medicine, Louisville, KY, USA

[3]Department of Medicine, University of Louisville, Louisville, KY, USA

[4]Department of Biochemistry and Molecular Genetics, University of Louisville, Louisville, KY, USA

[5]Leeds Thrombosis Collective, Department of Discovery and Translational Science, Leeds Institute of Cardiovascular and Metabolic Medicine, University of Leeds, UK

[6]Division of Experimental Hematology and Cancer Biology, Cincinnati Children's Hospital Medical Center, Cincinnati, OH, USA

Abstract

Factor XIIIA (FXIIIA) is a transglutaminase that crosslinks intra- and extracellular protein substrates. FXIIIA is expressed as an inactive zymogen, and during blood coagulation, it is activated by removal of an activation peptide by the protease thrombin. No such proteolytic FXIIIA activation is known to occur in other tissues or the intracellular form of FXIIIA. For those locations, FXIIIA is assumed instead to undergo activation by Ca^{2+} ions. Previously, we demonstrated a monomeric state for active FXIIIA. Current analytical ultracentrifugation and kinetic experiments revealed that thrombin-activated FXIIIA has a higher conformational flexibility and a stronger affinity toward glutamine substrate than does nonproteolytically activated FXIIIA. The proteolytic activation of FXIIIA was further investigated in a context of fibrin clotting. In a series of fibrin crosslinking assays and scanning electron microscopy studies of plasma clots, the activation rates of FXIIIA V34X variants was correlated with the extent of fibrin crosslinking and incorporation of nonfibrous protein into the clot. Overall, the results suggest conformational and functional differences between active FXIIIA forms, thus expanding the understanding of FXIIIA function. Those differences may serve as a basis for developing therapeutic strategies to target FXIIIA in different physiological environments.

To whom correspondence should be addressed: Muriel C. Maurer Ph.D. Department of Chemistry, University of Louisville, 2320 South Brook Street, Louisville, KY 40292. Tel: (502) 852-7008; Fax: (502) 852-8149; muriel.maurer@louisville.edu.

Author contributions BA and MM designed the research. HP, KS, and RA constructed the expression vectors for GST tagged FXIIIA V34 and Fbg αC (233-425) and also contributed to research planning. MF supplied the FXIIIA-deficient murine plasma (FXIII $A^{-/-}$) and guidance on its use. BA and WD carried out the experiments. BA and MM wrote the manuscript. All authors reviewed the data, and both critiqued and approved the manuscript.

Conflict of interest The authors state that they have no conflict of interests.

Enzymes: Factor XIIIA (**EC 2.3.2.13**).

Graphical Abstract

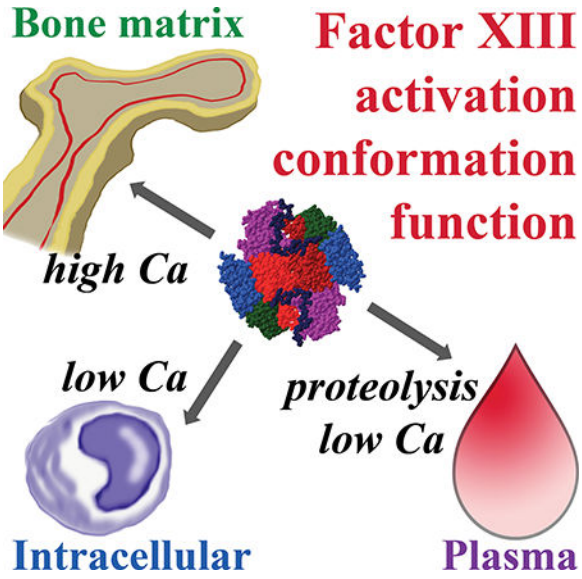

When Factor XIII undergoes 1) proteolytic activation with low mM Ca^{2+}, 2) slow, nonproteolytic activation with low mM Ca^{2+}, or 3) nonproteolytic activation at high mM Ca^{2+}, the resultant transglutaminases exhibit conformationally and functionally different enzymatic properties. These variations support development of therapeutic strategies to target FXIIIA in different physiological environments.

Keywords

Factor XIII; transglutaminase; fibrin clot; analytical ultracentrifugation; scanning electron microscopy

INTRODUCTION

Factor XIIIA (FXIIIA) has been a subject of medically related research for almost a century. Perhaps the most studied is the role of FXIIIA in crosslinking the fibrin network, making it more mechanically stable and resistant to fibrinolysis. As physiological knowledge on FXIII expands, it becomes apparent that beyond serving as a key player of the blood coagulation system, FXIIIA functions in wound healing, bone tissue dynamics, signaling, and other areas [1–10].

FXIIIA is a transglutaminase that crosslinks protein substrates via an isopeptide bond in a Ca^{2+}-dependent manner. FXIIIA is expressed as an inactive zymogen and in plasma, it circulates in a heterotetrameric complex with carrier FXIIIB (A_2B_2). During blood coagulation, plasma FXIII is activated by thrombin-mediated removal of N-terminal activation peptides (AP) from the A-subunits followed by binding of Ca^{2+} and dissociation of the B-subunits [11]. The active FXIIIA then introduces covalent crosslinks between polymerizing fibrin molecules and incorporates other proteins into the network, ultimately increasing mechanical stability of the resulting clot and its resistance to fibrinolysis [12].

Intracellularly, such as in platelets, monocytes, and macrophages, FXIII exists as an A_2-homodimer and is thought to undergo slow nonproteolytic activation in the presence of low available Ca^{2+} concentrations [13–15]. In this physiological compartment, FXIIIA is present in the cytoplasm, associates with membrane [10, 16], and even appears in the nucleus [17]. Activation and translocation of FXIIIA from the platelet cytoplasm to the platelet membrane does not require thrombin dependent steps. The minor amount of transglutaminase activity observed in a subsequent fibrin-platelet environment is proposed to be due to non-proteolytic activation of FXIII A_2 [18]. Some other intracellular functions of FXIIIA include reorganization of cytoskeletal proteins and chromatin remodeling [9]. FXIIIA is also secreted by osteoblasts into the extracellular matrix (ECM) [19], where it contributes to formation of the ECM itself and remodeling of the bone tissue [6, 16, 20]. Although a 37 kDa proteolytic fragment of FXIIIA was proposed to exist in the bone ECM [19, 21], it was later identified as transaldolase-1 that was immunoreactive with anti-FXIIIA antibody [22]. Thus, no evidence of proteolytic FXIIIA activation in bone ECM currently exists. However, with available ECM Ca^{2+} concentrations as high as 25 – 40 mM [23, 24], bone ECM FXIIIA may be activated by Ca^{2+} without proteolysis.

FXIIIA has also been implicated in pathological conditions such as thrombosis [25], inflammation, oncogenic events and diabetes [10], and arthritis [26]. Although FXIIIA is involved in an array of intra- and extracellular events, an in-depth understanding of FXIIIA activation and function in different physiological environments is lacking. With more knowledge, therapeutic strategies might be developed to target zymogen FXIII or activated FXIIIA under specific physiological or pathological conditions. Previously, we studied the oligomeric states of FXIIIA in different solution conditions [27]. We found that FXIII A_2-homodimer dissociates into monomers during activation by thrombin. Cleavage of a single AP on the dimeric FXIII A_2 was sufficient to promote dissociation and full activity of the A-subunits. Nonproteolytic activation by high Ca^{2+} concentration also resulted in subunit dissociation, however, these species possessed lower activity [27].

In the current project, we hypothesized that in different physiological compartments such as blood plasma, intracellular, and bone ECM, activation of FXIIIA may result in conformationally different enzymatic species. We focused on probing functional implications of thrombin activation of FXIIIA in the presence of low mM Ca^{2+} (mimicking conditions in plasma, the resulting active species are henceforth denoted as FXIIIA*), nonproteolytic activation by low mM Ca^{2+} (intracellular activation, FXIIIA$^{\circ,low}$), and activation in the presence of high (≥25 mM) Ca^{2+} (bone ECM, FXIIIA$^{\circ,high}$). We demonstrated an overall slower rate of FXIIIA nonproteolytic activation, as compared to the thrombin-mediated cleavage. Moreover, enzymatic activity assays revealed differences in the substrate affinities of FXIIIA* and FXIIIA$^{\circ,high}$. Using a fibrin clotting model in a purified protein system as well as in plasma, we further examined how proteolytic activation of FXIIIA V34X variants can be used to control the rate of fibrin crosslinking function and also influence fibrin clot structure. In summary, our results support proposed conformational differences between FXIIIA active forms in different physiological environments. Finally, we discuss how these differences may serve as a basis for differential therapeutic targeting of FXIIIA.

RESULTS

Solution properties of FXIIIA species in different activation conditions

Previously in a series of AUC experiments, we demonstrated that zymogenic FXIII A_2 homodimer completely dissociates into monomers upon proteolytic and nonproteolytic activation [27]. In the current work, we employed sedimentation velocity AUC to compare the solution dynamics of FXIIIA under different conditions. FXIIIA was activated in the presence of 100 mM Ca^{2+} (FXIIIA$^{\circ,high}$) or by thrombin in the presence of 4 mM Ca^{2+} (FXIIIA*). The high 100 mM Ca^{2+} helped to quickly obtain uniform, monomeric FXIIIA $^{\circ,high}$ species [27]. As a control for a possible divalent cation-mediated ionic strength effect, additional samples of FXIIIA* were supplemented with 100 mM Mg^{2+}. Unlike Ca^{2+}, this divalent cation does not efficiently support dissociation or activity of FXIII A-subunits [27]. To eliminate possible differences in sample handling between separate analytical runs, all sample conditions were subjected to AUC at the same time. The resulting sedimentation coefficient distributions are presented in Fig. 1A. In the presence of 100 mM Ca^{2+} (FXIIIA $^{\circ,high}$, trace i), we observed a tall narrow peak, approximately 1 S unit in width. As reported previously [27], significant precipitation occurred in FXIIIA* samples during centrifugation, and the sedimentation distribution peak was much broader, approximately 2 S (trace ii). In the presence of 4 mM Ca^{2+} and 100 mM Mg^{2+} (trace iii), the FXIIIA* sedimentation peak was also broad (2 S).

Sedimentation coefficients represent the velocity of particle sedimentation (in the present case, FXIIIA molecules) in a centrifugal field [28]. Apart from the physical characteristics of a solution, which are accounted for in data analysis, the sedimentation coefficient ultimately depends on the weight and shape of those particles. Thus, in samples of monomeric FXIIIA, it is the diversity of shapes (conformations) that constitutes the sedimentation distribution. The broad sedimentation distribution peak indicates that FXIIIA* is more conformationally heterogeneous in solution than FXIIIA$^{\circ,high}$, and this heterogeneity is retained in the presence of 100 mM Mg^{2+}. This observation suggests that Ca^{2+} exerts a specific effect on FXIIIA conformation. The related divalent cation Mg^{2+} cannot mimic this property and, moreover, the conformational effect is not due to a simple increase in ionic strength.

To examine FXIIIA nonproteolytic activation at lower, more physiological Ca^{2+} concentrations, FXIIIA was incubated in the presence of 4 mM Ca^{2+} for 30 min – 96 h, followed by AUC. Unexpectedly, progressive precipitation was observed in these samples of FXIIIA$^{\circ,low}$, very similar to the solution behavior of the thrombin-activated FXIIIA*. In previous experiments, we found addition of 5% DMSO promoted solubility of FXIIIA* over the course of a few hours [27]. However, 4 mM Ca^{2+}-activation required longer incubation periods to obtain detectable results, and even addition of DMSO did not aid in full solubility of activated FXIIIA. The actual amount of protein in solution was assessed via absorbance at the start of an AUC experiment (Fig. 1B, insert). The plot in Fig. 1B (open circles) then represents the amount of monomeric FXIIIA as a fraction of soluble protein in each sample. The most observed dissociation of the A-subunits, ~ 65%, was observed after 72 h incubation. Such nonproteolytic activation of FXIIIA may proceed intracellularly, although

much slower than observed in the presence of 4 mM Ca^{2+}, as intracellular Ca^{2+} is actually maintained at nanomolar to micromolar levels. Furthermore, the aggregation propensity of FXIIIA°,low suggests its relatively short lifetime, in a good agreement with a study by Muszbek *et al.* [13], reporting a small, 6.5% of FXIIIA population within platelets being active.

In order to mimic activation conditions of bone tissue ECM, FXIIIA was incubated in the presence of higher, 25 mM Ca^{2+} for 30 min – 6 h (Fig. 1B, filled circles). The dissociation of the dimeric zymogen under these conditions occurred faster than at 4 mM Ca^{2+} (80% at 6 h of incubation) and, analogous to activation by 100 mM Ca^{2+}, no precipitation of these FXIII°,high species was observed (Fig. 1B, panel on the right). Thus, the current results indicate overall slower activation of FXIIIA by Ca^{2+} alone, as compared to the proteolysis by thrombin resulting in full dissociation of FXIIIA within minutes. High (≥25 mM) Ca^{2+} levels reduce conformational heterogeneity and aid in maintaining stability of activated FXIIIA species in solution.

A model system of FXIIIA proteolytic activation kinetics

To better understand FXIIIA function in different physiological contexts, the peculiarities of individual activation environments need to be considered. Due to highly regulated calcium homeostasis in the body, nonproteolytic activation pathways leading to FXIIIA°,low and FXIIIA°,high likely operate on an ongoing basis. There will thus be slow, constitutive FXIII activity occurring within cells and ECM. Faster activation may then be achieved when higher Ca^{2+} concentrations are encountered as part of certain physiological or pathological processes. In blood plasma, where Ca^{2+} concentration is maintained at a low 1.5 mM, such constitutive generation of FXIIIA°,low is prevented by association of FXIIIA with the inhibitory FXIIIB [15]. Under exigent cases such as bleeding, the proteolytic removal of AP facilitates fast FXIIIA activation. The concomitant use of thrombin to activate FXIIIA and to convert fibrinogen to polymerizing fibrin adds complexity to this clotting mechanism [29]. As a result, the kinetics of FXIIIA* generation has a significant impact on the functional outcome of the clotting process.

To explore this outcome, we generated and expressed FXIIIA variants with different amino acid residues at position 34 of the FXIII activation peptide. These variants differ in their rate of cleavage by thrombin [30] (Fig. 2A). The current studies provided the first testing of AP residues F34 and W34 on FXIIIA proteolytic activation and resulting transglutaminase function. Using an extended range of FXIII activation rates, comparisons could be made with the naturally occurring V34 and L34. The FXIIIA AP variants were combined with human FXIII-free fibrinogen and clotting was initiated by addition of thrombin and Ca^{2+}. As expected, the rate of FXIIIA proteolytic activation determined development of FXIIIA* crosslinking activity (Fig. 2B). The fastest cleaved FXIIIA L34 generated both γ–γ and higher molecular weight (HMW) fibrin species already at an early stage (5 min) of the experiment. Slow cleavage of FXIIIA W34 by thrombin resulted in the slowest appearance of γ–γ and very little HMW crosslinks. Interestingly, F34 FXIIIA is cleaved by thrombin slightly slower than V34 variant (Fig. 2A); however, both variants crosslinked fibrin to a similar extent. This effect may be explained by the fact that the cleavage of a single AP on

dimeric FXIIIA zymogen results in dissociation and promotes full activity of both cleaved and noncleaved A-subunits [27, 31]. In addition, a competition of fibrinogen and FXIIIA for thrombin may have further masked the difference in V34 and F34 cleavage rate observed in the absence of fibrinogen. The four full-length FXIII V34X variants could thus be used to control the timing of appearance of FXIII activity without diminishing thrombin-mediated conversion of fibrinogen to fibrin or altering the clot gelation dynamics. Moreover, the extent of crosslinking before initiation of fibrinolysis could be documented.

To further probe the functional impact of FXIIIA activation rate, three AP variants that demonstrated different degrees of fibrin crosslinking (L34, V34, and W34) were introduced into FXIIIA-deficient murine plasma, and clotting was initiated by addition of thrombin and Ca^{2+}. The murine plasma system was already well established for introducing and screening FXIII V34, V34L, and/or G33A based clotting effects [32–34]. The resulting clots were imaged by SEM and representative photographs are shown in Fig. 3. Clots formed in the presence of FXIIIA better retained their three-dimensional structure due to FXIIIA-mediated covalent crosslinking of the fibrin fibers. Interestingly, we observed nonfibrous protein networks embedded to different degrees within the crosslinked fibrin clots. The least amount occurred with the FXIII AP- variant W34 (slower proteolytic activation) and the most with the L34 (faster activation). Such networks were uniformly distributed and must be covalently crosslinked within the clot, since they remained even after extensive washing during SEM sample preparation. The nonfibrous material may represent unpolymerized fibrin or other plasma proteins and is expected to contribute to overall clot penetrability and mechanical and fibrinolytic stability.

Catalytic comparisons of FXIIIA* and FXIIIA$^{\circ,high}$

Previously, when using a standard coupled ammonia release assay [35], we observed lower catalytic activity for FXIIIA$^{\circ,high}$, as compared to FXIIIA* [27]. In the current work, we attempted to probe this difference in more detail. The transglutaminase activities of FXIIIA activated by thrombin in the presence of 4 mM Ca^{2+} (FXIIIA*) or by 100 mM Ca^{2+} (FXIIIA$^{\circ,high}$) were compared in a series of enzymatic evaluations. Since it was impossible to isolate stable, uniformly monomeric species of FXIII$^{\circ,low}$ on a reasonable time scale, this FXIIIA form was not included in catalytic comparisons.

To assess the catalytic differences between FXIIIA* and FXIII$^{\circ,high}$, we employed a spectrophotometric assay using K9 peptide (^{1}LGPGQSKVIG^{10}) as a glutamine substrate and chromogenic DMPDA as second, amine substrate. Unlike the ammonia release assay, the transglutaminase reaction was now monitored directly at its second step, formation of a cross-linked product. An apparent K_m for K9 peptide was almost two-fold lower for FXIIIA*, compared to FXIIIA$^{\circ,high}$. This lower K_m indicated better interaction of the FXIIIA* enzymatic form with the glutamine substrate (Fig. 4A). On the other hand, FXIII$^{\circ,high}$ demonstrated a slightly stronger V_{max} value suggesting that once saturated with the glutamine donor K9, FXIII$^{\circ,high}$ provides faster substrate turnover than FXIIIA*. Thus, the observed individual kinetic parameters further corroborate proposed conformational/dynamic differences between FXIIIA* and FXIIIA$^{\circ,high}$.

We next conducted a series of SDS-PAGE assays to monitor FXIIIA-catalyzed crosslinking of a lysine mimic monodansylcadaverine (MDC) to a glutamine donor fibrinogen αC (233–425). The dansyl moiety of MDC provides a fluorescent tag on the protein and once the αC band is resolved on SDS-PAGE, the crosslinking reaction can be monitored by fluorescence of that band. αC represents a physiological FXIIIA protein substrate and contains three reactive glutamines [36]. While four lysine residues are present in the αC (233–425) sequence, no competing αC–αC conjugation, that would result in appearance of species of ≥40 kDa, was detected even at high αC concentrations (Fig. 4B, panel iv). At 5 μM αC concentration, the extent of MDC incorporation catalyzed by FXIIIA* was greater than by FXIIIA$^{\circ,high}$ (Fig. 4B, panel i). Interestingly, increased monovalent ionic strength has been shown to promote higher FXIIIA activity [13, 15, 37, 38]. To rule out the possibility of an inhibitory effect of divalent ionic strength, the Ca^{2+} concentration in the crosslinking reaction was lowered from 100 mM down to 25 mM Ca^{2+} (Fig. 4B, panel ii). MDC crosslinking to αC by FXIIIA$^{\circ,high}$ was essentially the same regardless of Ca^{2+} concentration in the crosslinking reaction mix, and in both cases, the FXIIIA$^{\circ,high}$ activity was lower than that catalyzed by FXIIIA*. When αC concentration was raised to 40 μM, the difference between crosslinking activity of FXIIIA* and FXIIIA$^{\circ,high}$ became indistinguishable (Fig. 4B, panel iii). Overall, the results obtained with the short K9 peptide and a larger, more physiological αC substrate, suggest that FXIIIA* interacts with the glutamine substrate more readily than does FXIIIA$^{\circ,high}$.

DISCUSSION

Factor XIII activity has been reported in a variety of intra- and extracellular physiological environments and has been implicated in numerous pathological events. Being the final player of the coagulation cascade, FXIIIA has been recognized as a promising target for novel anticoagulant agents, with a prospect of fewer side effects [25, 39–41]. When implementing new coagulation management regimes, it may be desirable not to affect FXIII function in nonhemostatic events. On the other hand, those nonhemostatic functions may themselves present therapeutic interest. It is important to keep in mind that FXIII is activated either proteolytically or non-proteolytically depending on the physiological environment. To support future pharmaceutical intervention approaches, critical new knowledge on these two FXIII activation strategies and their subsequent functional properties is needed.

Using AUC in previous work, we demonstrated dissociation of the FXIII A_2 dimer upon activation and that it is the monomeric FXIIIA that is catalytically competent [27]. In the current project, we investigated and compared dynamic and functional implications of proteolytic and nonproteolytic FXIIIA activation pathways. While thrombin-mediated proteolysis resulted in full dissociation of the A-subunits within minutes, activation by Ca^{2+} alone at physiological concentrations proceeded slower and took hours. Due to highly regulated Ca homeostasis, however, this activation pathway may operate constantly, thus providing constitutive FXIII activity within cells and ECM.

In contrast to FXIIIA* and FXIIIA$^{\circ,low}$, nonproteolytic activation in the presence of high (≥25 mM) Ca^{2+} did not result in aggregation of FXIIIA$^{\circ,high}$ species. Increased Ca^{2+} concentration was shown before to stabilize active FXIIIA in solution [31], and in current

AUC experiments, we correlated higher Ca^{2+} levels with reduced conformational heterogeneity of FXIIIA$^{\circ,high}$, as compared to FXIIIA*. The poor solubility of FXIIIA$^{\circ,low}$ may suggest partial conformational similarity with FXIIIA*. However, the slow appearance of this form has limited its isolation and characterization in the current study.

In our enzymatic evaluations, FXIIIA* had an almost two fold lower K_m for the glutamine substrate than had FXIIIA$^{\circ,high}$, thus suggesting stronger interaction of FXIIIA* with that substrate. On the other hand, FXIIIA$^{\circ,high}$ provided faster reaction turnover upon saturation with the glutamine donor. It is well known that the transglutaminase reaction proceeds through a mechanism involving addition of Q (glutamine) and K (amine or lysine) substrates. That is, the K-substrate enters the reaction after the enzyme forms a complex with the Q-substrate [42]. Therefore, this faster turnover by FXIIIA$^{\circ,high}$ may be due to better interaction with the K-substrate and faster release of the crosslinked product.

In early work, Lewis with coworkers [43] reported that each A-subunit of plasma zymogen FXIII A_2B_2 binds a Ca^{2+} ion with 100 μM K_D. Hornyak *et al.* [44] later demonstrated that another Ca^{2+} ion is required by each A-subunit to dissociate from the B-subunits and to expose catalytic cysteines. Stieler with coworkers [40] recently crystallized FXIIIA$^{\circ,high}$ with a covalently bound Q-mimic inhibitor, providing the first molecular structure of active FXIIIA. Besides the previously observed first, zymogenic Ca^{2+} site [45], the Stieler research group elegantly demonstrated the functional significance of two additional sites. In particular, development of the 2nd Ca^{2+} site brought about conformational changes in the FXIIIA molecule to initiate formation of a hydrophobic pocket for the K-substrate entrance. This site is the same as that presumed by Hornyak [44] to promote exposure of the reactive thiol on A-subunits. Coordination of the 3rd Ca^{2+} was proposed by Stieler *et al.* [40] to conclude formation of the hydrophobic pocket and to facilitate binding of the K-substrate.

Since the addition of Q and K is sequential and the crystal structure presented by Stieler *et al.* [40] depicts a covalent FXIIIA–Q-substrate intermediate rather than a free enzyme, we entertain an idea that the 3rd site for Ca^{2+} is filled upon binding of the Q-substrate. Whether binding of Ca^{2+} at the 3rd site precedes binding of the K-substrate or vice versa, is open to speculation. It seems plausible that at relatively low Ca^{2+} levels coordination of this 3rd site and completion of the hydrophobic pocket is dependent on the availability of the K-substrate. Such a possibility is consistent with the fact that in the absence of K-substrate, a water molecule acts as an acyl acceptor resulting in net deamidation of the glutamine to glutamate [46]. Intriguingly, the Ca^{2+} requirement for deamidation catalyzed by guinea pig liver transglutaminase was demonstrated to be much lower than that for transamidation (crosslinking) [47], further supporting this possibility for a homologous FXIIIA.

In conditions where Ca concentrations are relatively high, such as in bone ECM, the 3rd FXIIIA Ca^{2+} site may already be saturated even in a free enzyme, prior to the Q-substrate binding. Our kinetic results suggest that this saturation facilitates a conformation (FXIIIA $^{\circ,high}$) that has a weaker affinity for the Q-substrate (indicated by higher K_m in the current study) but provides faster reaction turnover, than FXIIIA* (higher observed V_{max}). In addition to its stabilizing role observed in our AUC experiments, the FXIIIA$^{\circ,high}$

conformation may also favor transamidation of the protein substrates over deamidation in acidic conditions of the bone ECM.

Thus far, the FXIIIA* form has been elusive from crystallographic efforts and also a challenging subject of solution experiments. The current studies effectively demonstrate that conformational differences do exist between FXIIIA* and FXIII$^{\circ,high}$. As mentioned before, the crystal structures of non-proteolytically activated FXIII$^{\circ,high}$ in complexes with inhibitors are available from the Stieler group (PDB 4KTY, 5MHM, 5MHN, 5MHO). It would thus be feasible to screen for pharmaceutical candidates that confer specificity to FXIIIA$^{\circ,high}$ and eliminate those affecting the FXIIIA*. Should this orthosteric design fail, a search for allosteric effectors may be more successful [41]. Previous studies in our group involving chemical modification and hydrogen-deuterium exchange suggested better solvent accessibility of the β-sandwich region of FXIIIA*, while β-barrel 1 was more solvent-exposed in FXIIIA$^{\circ,high}$ [48, 49]. These local structural differences may serve as a starting point for allosteric targeting of FXIIIA.

Prior studies have shown that increasing levels of FXIII A* affect the rate and extent of fibrin crosslinking [12, 33, 50]. Taking this property into consideration, the fibrin clot network could be further manipulated by regulating proteolytic activation of FXIII. In the current work, we showed that the FXIII V34X variants (L34, F34, and W34) influenced such FXIIIA* generation rates and in response affected fibrin crosslinking. Faster proteolytic activation (and hence, higher amount of FXIIIA*) during blood coagulation resulted in a greater extent of fibrin crosslinking and incorporation of other proteins into the clot (FXIII L34>V34,F34>W34). The current results effectively complement FXIII activation peptide models examined by Duval and coworkers. Their studies focused on A34, L34, M34 along with surrounding FXIII AP residues [32]. Our focus has been on fast activating L34 versus aromatic V34X substitutions that are well tolerated by the anticoagulant thrombin W215A species [30]. Thus, therapeutic strategies to specifically limit thrombin's ability to activate FXIIIA and/or fibrinogen, may be promising. The tunable FXIII-based ^{34}**X**VPR↓G^{38} amino acid sequence might also be employed as a prodrug linker. Thrombin-dependent cleavage of the linker sequence would release the pharmaceutical agent at a desirable rate and specifically at the clotting site. This approach would also ensure that neither FXIIIA$^{\circ,low}$ nor FXIIIA$^{\circ,high}$ are affected.

Overall, the presented research expands the understanding of the functional outcomes of FXIII activation pathways. Based on our previous and current results, we offer the following model: nonproteolytic FXIIIA activation proceeds relatively slow, but constantly. High mM Ca^{2+} levels, such as in bone ECM, stabilize the FXIIIA$^{\circ,high}$ form and provide its constitutive activity as part of the tissue remodeling processes. By contrast, thrombin-mediated AP-removal facilitates binding of Ca^{2+} at its low level in plasma, thus promoting fast buildup of FXIII crosslinking activity. The resultant FXIIIA* species have higher affinity towards glutamine substrates and respond even to low concentrations of these substrates, ensuring clot-stabilizing function during blood coagulation. At the same time, the tendency of FXIIIA* to aggregation may determine its relatively short life time in plasma. Different activation conditions also result in conformationally different FXIIIA forms, thus

providing a possible basis for developing therapeutic strategies for compartment-specific management of FXIIIA function.

EXPERIMENTAL PROCEDURES

Materials

Recombinant yeast expressed FXIIIA was a gift from the late Dr. Paul Bishop (Zymogenetics, Seattle, WA, USA). Recombinant human thrombin was generously provided by Dr. Enrico Di Cera and Dr. Leslie Pelc (St. Louis University, MO, USA). Bovine thrombin was purchased from Sigma-Aldrich (USA). Human FXIII-free peak 1 fibrinogen was purchased from Enzyme Research Laboratories (South Bend, IN, USA). Murine plasma was obtained from mice lacking the FXIII catalytic A subunit (FXIII $A^{-/-}$) [26, 51]. Such FXIII-deficient mice were engineered to be missing the FXIII A subunits but still express the FXIII B subunits. These mice were maintained at the Cincinnati Children's Hospital Medical Center animal care facility. All studies involving the use of animals were approved by the Cincinnati Children's Hospital Medical Center Institutional Animal Care and Use Committee. Cincinnati Children's Hospital is an AAALAC accredited institution. Thrombin inhibitor *D*-phenylalanyl-prolyl-arginyl chloromethyl ketone (PPACK) was purchased from Haematologic Technologies (Essex Junction, VT, USA). A transglutaminase glutamine substrate peptide K9 (^{1}LGPGQSKVIG^{10}) was synthesized by New England Peptide (Gardner, MA, USA). All other reagents were of the highest purity available.

AUC studies of FXIIIA

Molar concentration in this work refers to A-subunits as opposed to A_2-dimers of FXIIIA. 2 μM zymogen FXIIIA was incubated in borate buffer (20 mM boric acid, pH 7.8, 150 mM NaCl) in the presence of 25 – 100 mM $CaCl_2$ for 30 min – 6 h at 37 °C. FXIIIA was also incubated in the borate buffer at a lower 4 mM $CaCl_2$ for 30 min – 96 h. To achieve better solubility of FXIIIA under these conditions, the 4 mM Ca^{2+}-samples were supplemented with 5% DMSO. For proteolytic activation, 2 μM FXIIIA was incubated in the borate buffer with bovine thrombin (3.5 NIH units/ml) and 4 mM $CaCl_2$ for 30 min at 37 °C, followed by inhibition of thrombin with 760 nM PPACK. In addition to 4 mM $CaCl_2$, some samples of the proteolytically activated FXIIIA were supplemented with 100 mM $MgCl_2$.

A detailed description of AUC experimental parameters can be found in [27]. Briefly, samples of activated FXIIIA were subjected to sedimentation velocity AUC in an Optima XL-A ultracentrifuge (Beckman Coulter) at 20 °C and 50,000 rpm. Data were analyzed using the program SEDFIT (www.analyticalultracentrifugation.com), and experimental sedimentation coefficients were corrected based on the measured density and viscosity of the buffer, thus allowing direct comparison of results obtained with different experimental conditions. Analytical runs were performed with two independent samples for each condition examined. Control studies repeated in the current project yielded Sedimentation Coefficient values that were highly comparable.

Expression and purification of FXIIIA V34X variants and Fibrinogen αC (233–425)

pGEX plasmid vectors encoding GST-tagged FXIIIA V34 and GST-tagged fibrinogen αC (233–425) were employed [52]. Single amino acid V34X substitutions (L, F, or W) were introduced into the GST-FXIIIA plasmid using the QuikChange II Mutagenesis kit (Agilent Technologies). The expression vectors were transformed into *E. coli* BL21 (DE3) Gold cells and proteins were expressed using auto-inducing media [53]. Using an AKTA Prime FPLC, GST-tagged proteins were purified by affinity chromatography on a GST-trap column (GE Healthcare, USA) system. Target proteins were cleaved from the GST-tag by in-column digestion with PreScission protease and eluted with tris buffered saline (TBS, Tris Acetate 50 mM, pH 7.4, NaCl 150 mM). The purity was assessed using SDS-PAGE, and molar concentration was determined from absorbance readings at 280 nm using ε = 125710 $M^{-1}cm^{-1}$ for V34, F34, L34 FXIIIA variants and 131210 $M^{-1}cm^{-1}$ for W34 FXIIIA. An ε = 41480 $M^{-1}cm^{-1}$ was applied for fibrinogen αC (233–425). These extinction coefficients were calculated using Protparam tool (www.expasy.org).

Fibrin crosslinking in the presence of FXIIIA V34X variants

Human FXIII-free fibrinogen (1 mg/ml), a recombinant FXIII AP variant (V34, L34, F34, or W34, 50 nM), and recombinant human thrombin (12 nM) were incubated in a 20 μL TBS containing 2.5 mM $CaCl_2$ at 37 °C. At each time point (5 – 60 min), the reaction was quenched by addition of 10 μL of reducing sample loading buffer followed by boiling for 5 min, resulting in full solubilization of formed clots. Samples were then subjected to SDS-PAGE on an 8% gel. These fibrin crosslinking results were confirmed in three independent experiments.

SEM analysis of plasma clots formed in the presence of FXIIIA V34X variaants

A recombinant FXIII AP variant (L34, V34, or W34, 100 nM final concentration) was administered into citrated plasma from FXIIIA-deficient mice. Our FXIII concentration (100 nM) is within the physiological range of 86–173 nM [54]. After 5 min incubation at 37 °C, clotting was initiated by addition of bovine thrombin (to a final concentration of 2.1 NIH units/ml) and $CaCl_2$ (final 13.5 mM, to exceed the citrate in plasma) in the borate buffer, resulting in a 1:4 dilution of the stock plasma. Clots were incubated for 2 h at 37 °C in closed microfuge tubes, rinsed with deionized H_2O, and dehydrated in the presence of increasing (10 – 100%) concentrations of ethanol and dried with hexamethyldisilazane. The samples were next sputter-coated with Au-Pd and imaged using a Zeiss Supra 35 electron microscope.

Since we aimed to study *FXIIIA-mediated* crosslinking of the fibrin clots, no glutaraldehyde (a chemical crosslinking agent) was used to stabilize the samples. Undiluted plasma clots suffered great deformation during drying and were too dense. A 1:4 dilution of the plasma (and hence, endogenous fibrinogen) resulted in thinner, more suitable SEM samples that allowed for adequate comparisons between exogenous FXIIIA variants. These experiments were performed in duplicate.

MDC crosslinking SDS-PAGE based activity assay

In order to compare activities of proteolytically and nonproteolytically activated FXIIIA, a series of MDC crosslinking assays was performed. For proteolytic activation, 1 μM FXIIIA was incubated in TBS with 30 nM recombinant human thrombin and 4 mM $CaCl_2$ for 30 min at 37 °C, followed by addition of 760 nM thrombin inhibitor PPACK. Nonproteolytic activation was achieved by 30 min incubation of 1 μM FXIIIA in TBS in the presence of 100 mM $CaCl_2$.

Recombinantly expressed fibrinogen αC (233–425) was used as a glutamine donor (Q-substrate). αC (5 – 40 μM final) was preincubated for 5 min at 37 °C with a lysine mimic MDC (K-substrate, 1 mM final, from a 20 mM stock solution in methanol) in TBS containing $CaCl_2$ (4 – 100 mM final concentration). The crosslinking was initiated by addition of activated FXIIIA (final concentration 100 nM). Reaction aliquots were taken at 1 – 7 min and quenched by addition of reducing sample loading buffer, followed by 3 min of boiling. Samples were resolved using SDS-PAGE on 15% gels. Prior to Coomassie blue staining, the gels were photographed under UV light. The different MDC assay series were performed three independent times with comparable results obtained each time.

Continuous spectrophotometric kinetic assay

In this assay adapted from de Macedo *et al.* [55], FXIIIA incorporated chromogenic K-substrate *N,N*-dimethyl-1,4-phenylenediamine (DMPDA) into a Q-substrate K9-peptide. The reaction progress was monitored by an increase in absorbance at 278 nm resulting from an anilide functionality of the crosslinked product. Nonproteolytic and proteolytic activation were performed as described for the MDC assay, except that FXIIIA was 4 μM in the activation mix. K9-peptide (46 – 1386 μM final) was preincubated with DMPDA (700 μM final, from a 100 mM stock solution in methanol) in the borate buffer with 4 or 100 mM of $CaCl_2$ for 5 min at 37 °C. The reaction was initiated by addition of activated FXIIIA (final concentration 1 μM). Reaction velocities were determined over the initial part of the absorbance curve. An $\varepsilon = 8940\ M^{-1}\ cm^{-1}$ [55] was applied to convert absorbance to μM of crosslinked product. Less than 15% of both Q and K substrates reacted in the initial linear region of the absorbance curves. Velocities in μM min^{-1} were fitted to the Michaelis-Menten equation as a function of the K9 concentrations using Kaleidagraph software (Synergy). The resultant K_m and V_{max} parameters represent apparent values and serve for comparison of nonproteolytically and proteolytically activated FXIIIA. The kinetic assays were performed in triplicate for each activation condition. Results are presented as mean ± SD.

Acknowledgements

The authors thank Dr. E. Di Cera and Dr. L. Pelc (St. Louis University) for generously supplying the recombinant human thrombin. We also appreciate tips for optimizing FXIIIA expression from Dr. J. Keillor and Dr. A. Mulani (University of Ottawa) and SEM support from Dr. E. Moiseeva (University of Louisville Huson Imaging and Characterization Facility). The authors thank R. Darul Amne Syed Mohammed for further review of the MDC assay design. In addition, we acknowledge F. D. Ablan and M. Hindi for helpful discussions of the manuscript. This research effort was performed in part at the Micro/Nano Technology Center (MNTC). The MNTC is a member of the National Science Foundation Manufacturing and Nano Integration Node, supported by ECCS-1542174. The research was supported by the National Institutes of Health grants R15 HL120068 (MCM) and R01 CA211098 (MJF), and by the British Heart Foundation grants RG/18/11/34036 (RASA) and PG/08/052/25172 (HP).

Abbreviations

FXIIIA	the A-subunit of coagulation Factor XIII
AP	Activation Peptide
ECM	extracellular matrix
FXIIIA*	Factor XIIIA activated by thrombin in the presence of 4 mM $CaCl_2$
FXIIIA°,low	Factor XIIIA activated nonproteolytically in the presence of 4 mM $CaCl_2$
FXIIIA°,high	Factor XIIIA activated nonproteolytically in the presence of ≥25 mM $CaCl_2$
PPACK	*D*-Phe-Pro-Arg chloromethyl ketone
AUC	analytical ultracentrifugation
DMSO	dimethyl sulfoxide
SEM	scanning electron microscopy
MDC	monodansylcadaverine
DMPDA	*N,N*-dimethyl-1,4-phenylenediamine

REFERENCES

1. Komaromi I, Bagoly Z & Muszbek L (2011) Factor XIII: novel structural and functional aspects, Journal of thrombosis and haemostasis : JTH. 9, 9–20. [PubMed: 20880254]
2. Muszbek L, Bereczky Z, Bagoly Z, Komaromi I & Katona E (2011) Factor XIII: a coagulation factor with multiple plasmatic and cellular functions, Physiological reviews. 91, 931–72. [PubMed: 21742792]
3. Schroeder V & Kohler HP (2016) Factor XIII: Structure and Function, Seminars in thrombosis and hemostasis. 42, 422–8. [PubMed: 27019464]
4. Eckert RL, Kaartinen MT, Nurminskaya M, Belkin AM, Colak G, Johnson GV & Mehta K (2014) Transglutaminase regulation of cell function, Physiol Rev. 94, 383–417. [PubMed: 24692352]
5. Hoac B, Nelea V, Jiang W, Kaartinen MT & McKee MD (2017) Mineralization-inhibiting effects of transglutaminase-crosslinked polymeric osteopontin, Bone. 101, 37–48. [PubMed: 28428079]
6. Mousa A, Cui C, Song A, Myneni VD, Sun H, Li JJ, Murshed M, Melino G & Kaartinen MT (2017) Transglutaminases factor XIII-A and TG2 regulate resorption, adipogenesis and plasma fibronectin homeostasis in bone and bone marrow, Cell Death Differ. 24, 844–854. [PubMed: 28387755]
7. Sun H & Kaartinen MT (2018) Transglutaminase activity regulates differentiation, migration and fusion of osteoclasts via affecting actin dynamics, J Cell Physiol. 233, 7497–7513. [PubMed: 29663380]
8. Dickneite G, Herwald H, Korte W, Allanore Y, Denton CP & Matucci Cerinic M (2015) Coagulation factor XIII: a multifunctional transglutaminase with clinical potential in a range of conditions, Thrombosis and haemostasis. 113, 686–97. [PubMed: 25652913]
9. Adany R & Bardos H (2003) Factor XIII subunit A as an intracellular transglutaminase, Cell Mol Life Sci. 60, 1049–60. [PubMed: 12861374]

10. Mitchell JL & Mutch NJ (2018) Let's cross-link: diverse functions of the promiscuous cellular transglutaminase, factor XIII-A, J Thromb Haemost.
11. Lorand L & Konishi K (1964) Activation of the fibrin stabilizing factor of plasma by thrombin, Arch Biochem Biophys. 105, 58–67. [PubMed: 14165504]
12. Hethershaw EL, Cilia La Corte AL, Duval C, Ali M, Grant PJ, Ariens RA & Philippou H (2014) The effect of blood coagulation factor XIII on fibrin clot structure and fibrinolysis, Journal of thrombosis and haemostasis : JTH. 12, 197–205. [PubMed: 24261582]
13. Muszbek L, Haramura G & Polgar J (1995) Transformation of cellular factor XIII into an active zymogen transglutaminase in thrombin-stimulated platelets, Thromb Haemost. 73, 702–5. [PubMed: 7495082]
14. Muszbek L, Polgar J & Boda Z (1993) Platelet Factor XIII becomes active without the release of activation peptide during platelet activation, Thromb Haemostasis. 69, 282–285. [PubMed: 8097064]
15. Polgar J, Hidasi V & Muszbek L (1990) Non-proteolytic activation of cellular protransglutaminase (placenta macrophage factor XIII), Biochem J. 267, 557–60. [PubMed: 1970724]
16. Al-Jallad HF, Myneni VD, Piercy-Kotb SA, Chabot N, Mulani A, Keillor JW & Kaartinen MT (2011) Plasma membrane factor XIIIA transglutaminase activity regulates osteoblast matrix secretion and deposition by affecting microtubule dynamics, PLoS One. 6, e15893. [PubMed: 21283799]
17. Adany R, Bardos H, Antal M, Modis L, Sarvary A, Szucs S & Balogh I (2001) Factor XIII of blood coagulation as a nuclear crosslinking enzyme, Thromb Haemost. 85, 845–51. [PubMed: 11372678]
18. Mitchell JL, Lionikiene AS, Fraser SR, Whyte CS, Booth NA & Mutch NJ (2014) Functional factor XIII-A is exposed on the stimulated platelet surface, Blood. 124, 3982–90. [PubMed: 25331118]
19. Piercy-Kotb SA, Mousa A, Al-Jallad HF, Myneni VD, Chicatun F, Nazhat SN & Kaartinen MT (2012) Factor XIIIA transglutaminase expression and secretion by osteoblasts is regulated by extracellular matrix collagen and the MAP kinase signaling pathway, J Cell Physiol. 227, 2936–46. [PubMed: 21959563]
20. Cui C, Wang S, Myneni VD, Hitomi K & Kaartinen MT (2014) Transglutaminase activity arising from Factor XIIIA is required for stabilization and conversion of plasma fibronectin into matrix in osteoblast cultures, Bone. 59, 127–38. [PubMed: 24246248]
21. Nakano Y, Al-Jallad HF, Mousa A & Kaartinen MT (2007) Expression and localization of plasma transglutaminase factor XIIIA in bone, J Histochem Cytochem. 55, 675–85. [PubMed: 17341477]
22. Cordell PA, Newell LM, Standeven KF, Adamson PJ, Simpson KR, Smith KA, Jackson CL, Grant PJ & Pease RJ (2015) Normal Bone Deposition Occurs in Mice Deficient in Factor XIII-A and Transglutaminase 2, Matrix Biol. 43, 85–96. [PubMed: 25680676]
23. Breitwieser GE (2008) Extracellular calcium as an integrator of tissue function, Int J Biochem Cell Biol. 40, 1467–80. [PubMed: 18328773]
24. Breuksch I, Weinert M & Brenner W (2016) The role of extracellular calcium in bone metastasis, J Bone Oncol. 5, 143–145. [PubMed: 27761377]
25. Wolberg AS (2018) Fibrinogen and factor XIII: newly recognized roles in venous thrombus formation and composition, Curr Opin Hematol. 25, 358–364. [PubMed: 29994896]
26. Raghu H, Cruz C, Rewerts CL, Frederick MD, Thornton S, Mullins ES, Schoenecker JG, Degen JL & Flick MJ (2015) Transglutaminase factor XIII promotes arthritis through mechanisms linked to inflammation and bone erosion, Blood. 125, 427–37. [PubMed: 25336631]
27. Anokhin BA, Stribinskis V, Dean WL & Maurer MC (2017) Activation of factor XIII is accompanied by a change in oligomerization state, The FEBS journal. 284, 3849–3861. [PubMed: 28915348]
28. Lebowitz J, Lewis MS & Schuck P (2002) Modern analytical ultracentrifugation in protein science: a tutorial review, Protein Sci. 11, 2067–79. [PubMed: 12192063]
29. Brummel KE, Butenas S & Mann KG (1999) An integrated study of fibrinogen during blood coagulation, J Biol Chem. 274, 22862–70. [PubMed: 10428872]

30. Jadhav MA, Goldsberry WN, Zink SE, Lamb KN, Simmons KE, Riposo CM, Anokhin BA & Maurer MC (2017) Screening cleavage of Factor XIII V34X Activation Peptides by thrombin mutants: A strategy for controlling fibrin architecture, Biochimica et biophysica acta. 1865, 1246–1254. [PubMed: 28687225]
31. Hornyak TJ, Bishop PD & Shafer JA (1989) Alpha-thrombin-catalyzed activation of human platelet factor XIII: relationship between proteolysis and factor XIIIa activity, Biochemistry. 28, 7326–32. [PubMed: 2819071]
32. Duval C, Ali M, Chaudhry WW, Ridger VC, Ariens RA & Philippou H (2016) Factor XIII A-Subunit V34L Variant Affects Thrombus Cross-Linking in a Murine Model of Thrombosis, Arteriosclerosis, thrombosis, and vascular biology. 36, 308–16.
33. Kattula S, Byrnes JR, Martin SM, Holle LA, Cooley BC, Flick MJ & Wolberg AS (2018) Factor XIII in plasma, but not in platelets, mediates red blood cell retention in clots and venous thrombus size in mice, Blood Adv. 2, 25–35. [PubMed: 29344582]
34. Byrnes JR, Wilson C, Boutelle AM, Brandner CB, Flick MJ, Philippou H & Wolberg AS (2016) The interaction between fibrinogen and zymogen FXIII-A2B2 is mediated by fibrinogen residues gamma390–396 and the FXIII-B subunits, Blood. 128, 1969–1978. [PubMed: 27561317]
35. Fickenscher K, Aab A & Stuber W (1991) A photometric assay for blood coagulation factor XIII, Thromb Haemost. 65, 535–40. [PubMed: 1871715]
36. Mouapi KN, Bell JD, Smith KA, Ariens RA, Philippou H & Maurer MC (2016) Ranking reactive glutamines in the fibrinogen alphaC region that are targeted by blood coagulant factor XIII, Blood. 127, 2241–8. [PubMed: 26951791]
37. Woofter RT & Maurer MC (2011) Role of calcium in the conformational dynamics of factor XIII activation examined by hydrogen-deuterium exchange coupled with MALDI-TOF MS, Archives of biochemistry and biophysics. 512, 87–95. [PubMed: 21640701]
38. Curtis CG, Stenberg P, Brown KL, Baron A, Chen K, Gray A, Simpson I & Lorand L (1974) Kinetics of transamidating enzymes. Production of thiol in the reactions of thiol esters with fibrinoligase, Biochemistry. 13, 3257–62. [PubMed: 4841063]
39. Heil A, Weber J, Buchold C, Pasternack R & Hils M (2013) Differences in the inhibition of coagulation factor XIII-A from animal species revealed by Michael Acceptor- and thioimidazol based blockers, Thromb Res. 131, e214–22. [PubMed: 23498170]
40. Stieler M, Weber J, Hils M, Kolb P, Heine A, Buchold C, Pasternack R & Klebe G (2013) Structure of active coagulation factor XIII triggered by calcium binding: basis for the design of next-generation anticoagulants, Angewandte Chemie. 52, 11930–4. [PubMed: 24115223]
41. Al-Horani RA, Karuturi R, Lee M, Afosah DK & Desai UR (2016) Allosteric Inhibition of Factor XIIIa. Non-Saccharide Glycosaminoglycan Mimetics, but Not Glycosaminoglycans, Exhibit Promising Inhibition Profile, PLoS One. 11, e0160189. [PubMed: 27467511]
42. Folk JE (1983) Mechanism and basis for specificity of transglutaminase-catalyzed epsilon-(gamma-glutamyl) lysine bond formation, Adv Enzymol Relat Areas Mol Biol. 54, 1–56. [PubMed: 6133417]
43. Lewis BA, Freyssinet JM & Holbrook JJ (1978) An equilibrium study of metal ion binding to human plasma coagulation factor XIII, Biochem J. 169, 397–402. [PubMed: 629762]
44. Hornyak TJ & Shafer JA (1991) Role of calcium ion in the generation of factor XIII activity, Biochemistry. 30, 6175–82. [PubMed: 2059625]
45. Yee VC, Le Trong I, Bishop PD, Pedersen LC, Stenkamp RE & Teller DC (1996) Structure and function studies of factor XIIIa by x-ray crystallography, Semin Thromb Hemost. 22, 377–84. [PubMed: 8989820]
46. Keillor JW, Clouthier CM, Apperley KY, Akbar A & Mulani A (2014) Acyl transfer mechanisms of tissue transglutaminase, Bioorg Chem. 57, 186–97. [PubMed: 25035302]
47. Folk JE, Cole PW & Mullooly JP (1968) Mechanim of action of guinea pig liver transglutaminase. V. The hydrolysis reaction, J Biol Chem. 243, 418–27. [PubMed: 5635784]
48. Turner BT, Sabo TM, Wilding D & Maurer MC (2004) Mapping of factor XIII solvent accessibility as a function of activation state using chemical modification methods, Biochemistry. 43, 9755–9765. [PubMed: 15274630]

49. Sabo TM, Brasher PB & Maurer MC (2007) Perturbations in factor XIII resulting from activation and inhibition examined by solution based methods and detected by MALDI-TOF MS, Biochemistry. 46, 10089–101. [PubMed: 17691819]
50. Shemirani AH, Haramura G, Bagoly Z & Muszbek L (2006) The combined effect of fibrin formation and factor XIII A subunit Val34Leu polymorphism on the activation of factor XIII in whole plasma, Biochimica et biophysica acta. 1764, 1420–3. [PubMed: 16920044]
51. Palumbo JS, Barney KA, Blevins EA, Shaw MA, Mishra A, Flick MJ, Kombrinck KW, Talmage KE, Souri M, Ichinose A & Degen JL (2008) Factor XIII transglutaminase supports hematogenous tumor cell metastasis through a mechanism dependent on natural killer cell function, Journal of thrombosis and haemostasis : JTH. 6, 812–9. [PubMed: 18315549]
52. Smith KA, Adamson PJ, Pease RJ, Brown JM, Balmforth AJ, Cordell PA, Ariens RA, Philippou H & Grant PJ (2011) Interactions between factor XIII and the alphaC region of fibrinogen, Blood. 117, 3460–8. [PubMed: 21224475]
53. Studier FW (2005) Protein production by auto-induction in high density shaking cultures, Protein expression and purification. 41, 207–34. [PubMed: 15915565]
54. Katona E, Haramura G, Karpati L, Fachet J & Muszbek L (2000) A simple, quick one-step ELISA assay for the determination of complex plasma factor XIII (A2B2), Thrombosis and haemostasis. 83, 268–73. [PubMed: 10739385]
55. de Macedo P, Marrano C & Keillor JW (2000) A direct continuous spectrophotometric assay for transglutaminase activity, Anal Biochem. 285, 16–20. [PubMed: 10998259]

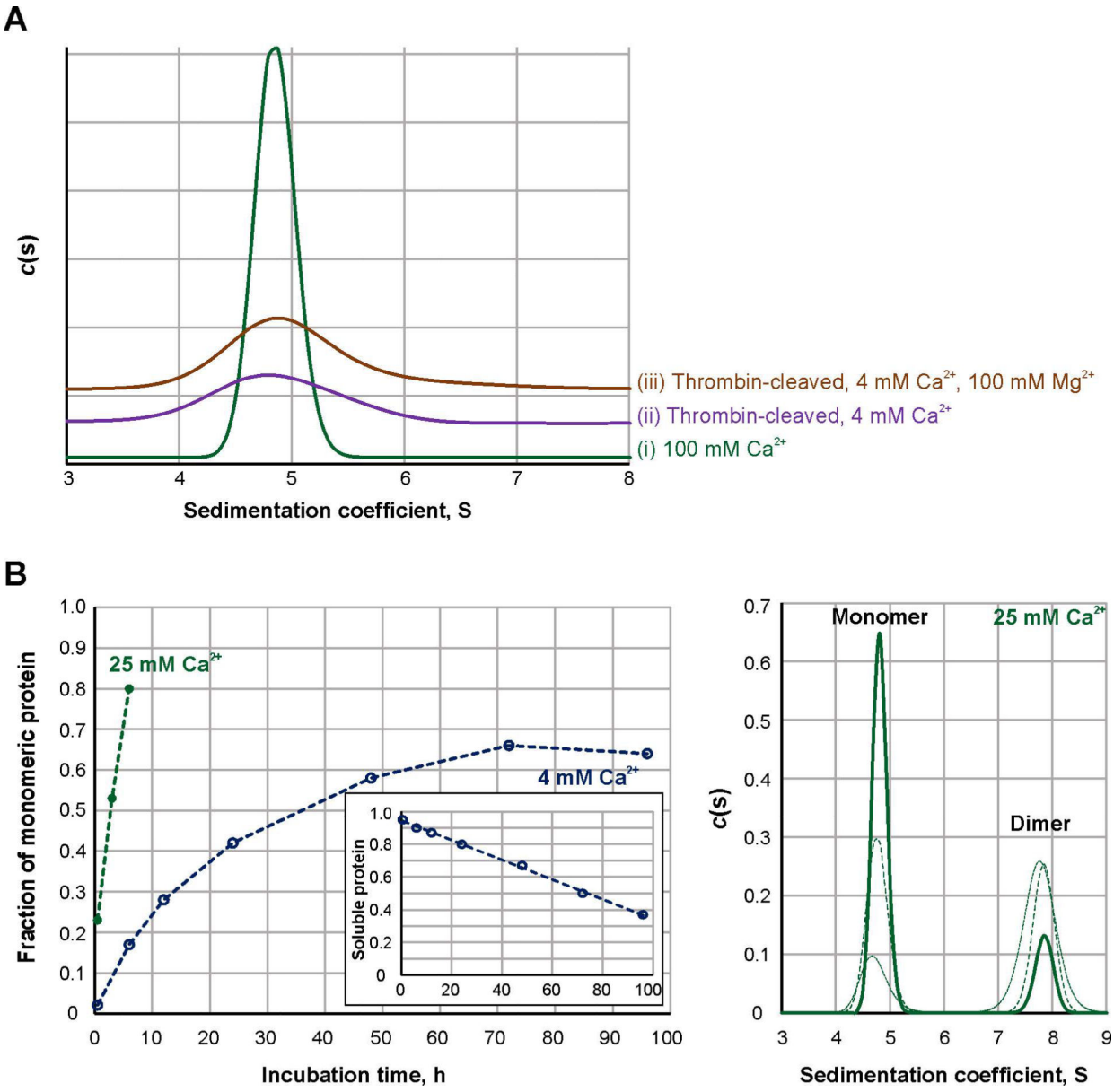

Fig. 1. Sedimentation properties and activation rate of FXIIIA under different conditions.

A – Sedimentation profiles of FXIIIA studied by AUC: 2 μM FXIIIA was activated at 37 °C for 30 min nonproteolytically by 100 mM $CaCl_2$ (trace I, green) or proteolytically by 3.5 NIH units/ml bovine thrombin in the presence of 4 mM $CaCl_2$ (trace ii, purple). An additional sample of thrombin-activated FXIIIA contained 4 mM $CaCl_2$ and 100 mM $MgCl_2$ (trace iii, orange). Two independent samples were analyzed for each condition, with the same results. (N=2)

B – Dissociation progress of 2 μM FXIIIA in the presence of 4 (open blue circles) and 25 mM $CaCl_2$ (filled green circles). Graph on the left presents quantitative analysis of sedimentation velocity AUC data. The insert demonstrates fraction of soluble protein (estimated from absorbance at 280 nm) in samples of 4 mM Ca^{2+}-activated FXIIIA as a function of time. The panel on the right depicts AUC sedimentation profiles for the FXIIIA

samples incubated in the presence of 25 mM $CaCl_2$ for 30 min (dotted green line), 3 h (dashed green line) and 6 h (solid green line).

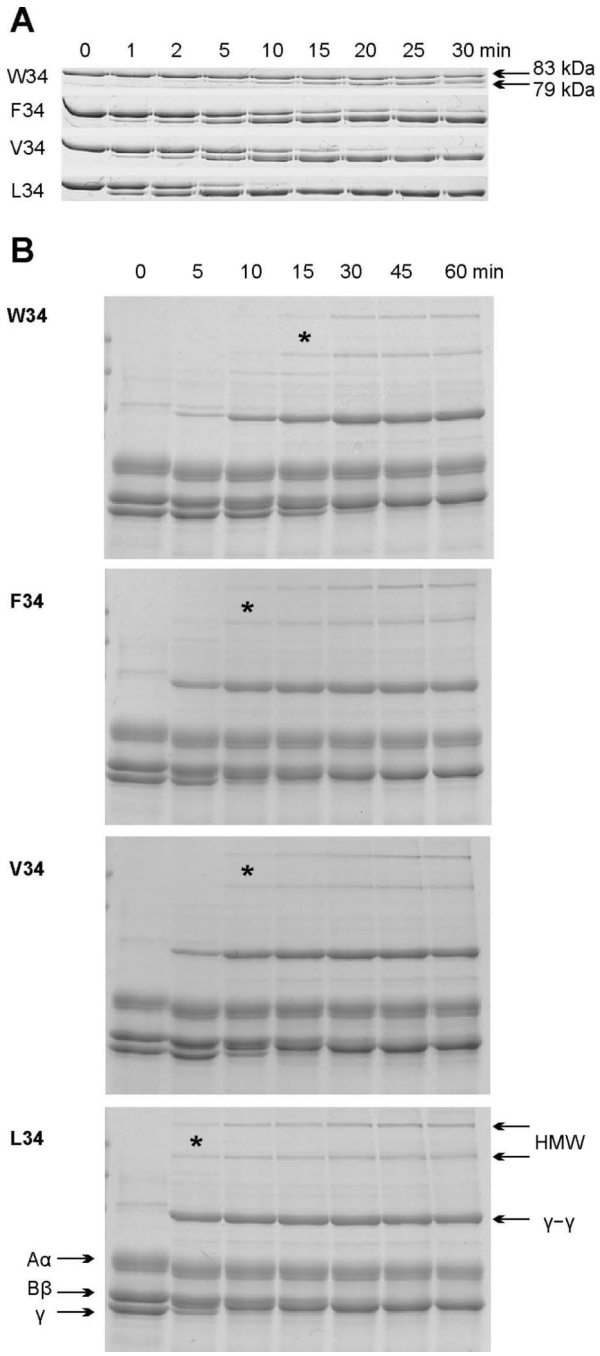

Fig. 2. Effect of the rate of FXIIIA proteolytic activation on fibrin crosslinking.

A – 1 μM recombinant FXIIIA AP variants were incubated with 30 nM recombinant human thrombin at 37 °C. Aliquots were withdrawn at denoted time points and thrombin was inhibited with 760 nM PPACK. The samples were then subjected to SDS-PAGE on 8% gels. FXIIIA AP cleavage resulting in a 4 kDa molecular weight loss could then be followed by monitoring the appearance of a 79 kDa band. (N=3)

B – Fibrin crosslinking by FXIIIA AP variants. 1 mg/ml human FXIII-free fibrinogen was combined with a recombinant FXIIIA AP-variant (50 nM) at 37 °C, and crosslinking was

initiated by addition of 12 nM recombinant human thrombin and 2.5 mM $CaCl_2$. At each denoted time point, the reaction was stopped by addition of reducing sample loading buffer and boiling. The samples were resolved via SDS-PAGE (8% gel). Fibrinogen chains Aα, Bβ, γ, HMW (high molecular weight crosslinks), and γ–γ crosslinks are annotated. * symbol denotes the earliest detection of HMW species during the course of the crosslinking reaction. (N = 3)

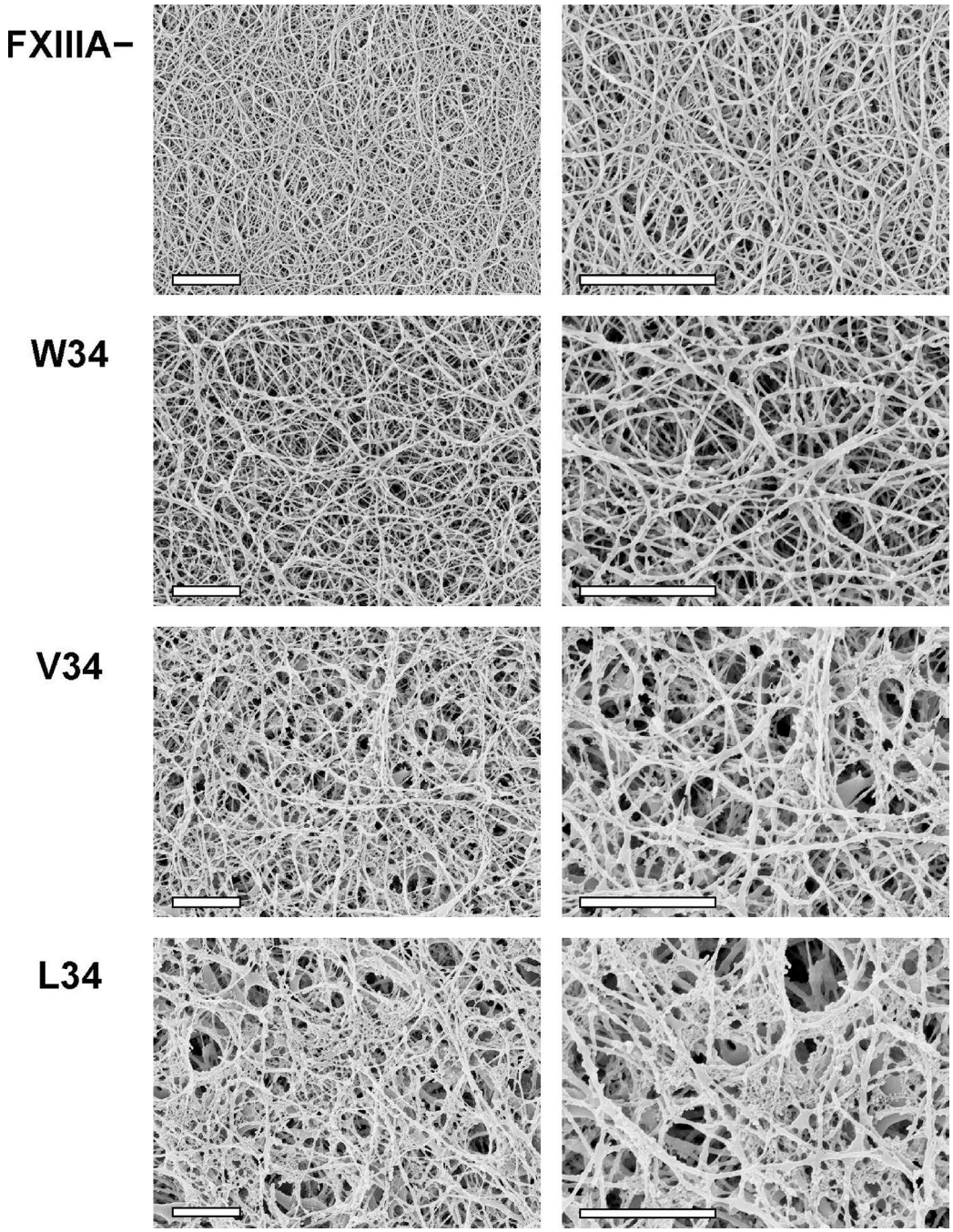

Fig. 3. Scanning electron microscopy of fibrin clots in the presence of FXIIIA AP variants.

100 nM FXIIIA AP variants were combined with plasma from FXIIIA-deficient mice (final dilution of plasma was 1:4). Control samples were made without FXIIIA (FXIIIA $^{-}$). Clotting was initiated by addition of 2.1 NIH units/ml bovine thrombin and 13.5 mM $CaCl_2$. Clots were formed for 2 h at 37 °C and prepared for SEM as described in Materials and Methods. For each FXIIIA AP variant, two clots were studied, with essentially the same results. Each set of clots (FXIII $^{-}$, W34, V34, and L34) was formed using plasma obtained from the same mouse. Shown are representative SEM photographs at two magnifications:

10,000x (left) and 20,000x (right), scale bars are 2 μm. Note that during the SEM sample preparation process, the fixative agent glutaraldehyde was not included to avoid artificial protein crosslinking. As a result, the FXIIIA$^-$ clots were significantly flattened during the dehydration process. In response, the resultant FXIIIA$^-$ fibrin fibers on the SEM images appeared denser packed.

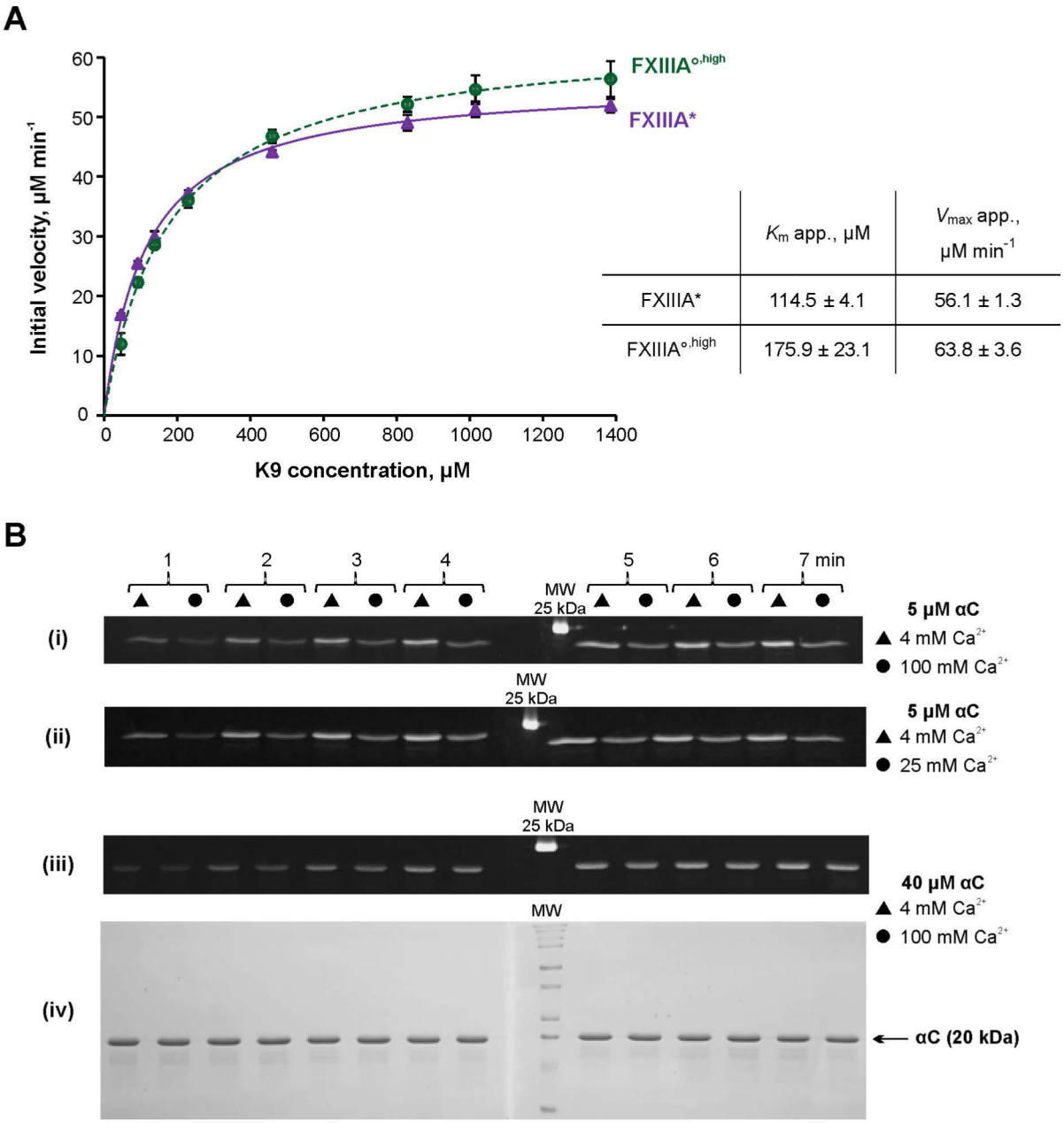

	K_m app., μM	V_{max} app., μM min^{-1}
FXIIIA*	114.5 ± 4.1	56.1 ± 1.3
FXIIIA°,high	175.9 ± 23.1	63.8 ± 3.6

Fig. 4. Transglutaminase activity of FXIIIA under different conditions.

A – Spectrophotometric kinetic assay. Glutamine donor K9 peptide was preincubated with the lysine mimic DMPDA at 37 °C for 5 min, and the crosslinking reaction was initiated by addition of 1 μM FXIIIA°,high (green circle) or FXIIIA* (purple circle). The reaction was followed by an increase in absorbance at 278 nm due to formation of the anilide crosslinked product. The plot represents Michaelis-Menten fits of the initial reaction velocities as function of the K9 concentration. Apparent K_m and V_{max} resulting from the fits are shown in the table insert. Values are presented as mean ± SD (N=3).

B – MDC crosslinking SDS-PAGE based assay. Recombinant fibrinogen αC (233–425) was preincubated with 1 mM MDC at 37 °C for 5 min. The crosslinking reaction was initiated by addition of 100 nM FXIIIA°,high or FXIIIA*. Reaction aliquots were withdrawn at 1 – 7 min

and quenched by addition of reducing sample buffer and boiling. The time point samples were loaded on 15% SDS-PAGE side by side for FXIIIA* (triangles) and FXIIIA$^{\circ,high}$ (circles). Two gels were run (1 – 4 and 5 – 7 min time points). The gels were aligned and photographed under UV light (panels i – iii). Panel iv – Coomassie Blue-stained gel pair from panel iii demonstrating absence of αC–αC conjugation. FXIIIA* was always preactivated in the presence of 4 mM $CaCl_2$, and FXIIIA$^{\circ,high}$ was preactivated in the presence of 100 mM $CaCl_2$. Concentrations of αC and $CaCl_2$ in the crosslinking reaction mix are annotated on the right. The different MDC assay series were performed three independent times.